IOP Publishing Journal of Physics: Condensed Matter
J. Phys.: Condens. Matter **27** (2015) 064104 (7pp) doi:10.1088/0953-8984/27/6/064104

The influence of DNA shape fluctuations on fluorescence resonance energy transfer efficiency measurements in nucleosomes

Lucia Lenz,[1,2] **Maurice Hoenderdos,**[1] **Peter Prinsen**[1] **and Helmut Schiessel**[1]

[1] Instituut-Lorentz, Leiden University, PO Box 9506, 2300 RA Leiden, The Netherlands
[2] Freiburg Institute for Advanced Studies (FRIAS), Albert-Ludwigs-Universität Freiburg, Albertstr. 19, 79104 Freiburg im Breisgau, Germany

E-mail: schiessel@lorentz.leidenuniv.nl

Received 19 May 2014, revised 30 June 2014
Accepted for publication 9 July 2014
Published 7 January 2015

Abstract

Fluorescence resonance energy transfer (FRET) measurements allow one to observe site exposure in nucleosomes, i.e. the transient unwrapping of a part of the wrapped DNA from the histone octamer. In such experiments one can typically distinguish between a closed state and an open state but in principle one might hope to detect several states, each corresponding to a certain number of open binding sites. Here we show that even in an ideal FRET setup it would be hard to detect unwrapping states with intermediate levels of FRET efficiencies. As the unwrapped DNA molecule, modelled here as a wormlike chain, has a finite stiffness, shape fluctuations smear out FRET signals completely from such intermediate states.

Keywords: DNA, nucleosome, FRET

(Some figures may appear in colour only in the online journal)

1. Introduction

In eukaryotic cells the DNA molecules are wrapped around protein cylinders forming so-called nucleosomes, the basic repeat unit of the chromatin complex. In a nucleosome 147 base pairs (bp) of DNA are wrapped along a left-handed superhelical wrapping path in one and three quarter turns around an octamer of histone proteins [1]. The main contribution to the DNA-histone interaction is localised at 14 binding sites where the minor groove of the DNA faces the octamer. The biophysical properties of nucleosomes can nowadays be probed via diverse experimental methods. We focus here on fluorescence resonance energy transfer (FRET) as a means to detect transient DNA unwrapping in nucleosomes.

The Widom group [2–6] demonstrated first that the nucleosome is a dynamic structure with parts of its DNA spontaneously unwrapping from either of its ends. They speculated that this site exposure mechanism gives DNA binding proteins access to target sequences if they happen to be located inside a nucleosome. In fact, in the experiments the accessibility for restriction enzymes was measured directly. It was found that the access to the restriction sites is more reduced the deeper the site is buried inside the nucleosome. A theoretical analysis of this experiment [7, 8] estimated that the net adsorption energy per binding site is about $1\,k_{\mathrm{B}}T$ where k_{B} is Boltzmann's constant and T is the temperature. This suggests that the attraction to the histone core has been tuned to just overcome the huge bending cost for the DNA wrapping, thereby allowing for spontaneous opening fluctuations.

Nowadays one can follow the unwrapping dynamics more directly with the help of FRET. In such experiments a donor and an acceptor dye are attached to the DNA and to the octamer [9–14] or both to the DNA molecule [15–25]. In all the experiments the donor and acceptor are positioned in a such way that they are close to each other for a completely wrapped nucleosome, leading to a FRET signal. On the other hand,

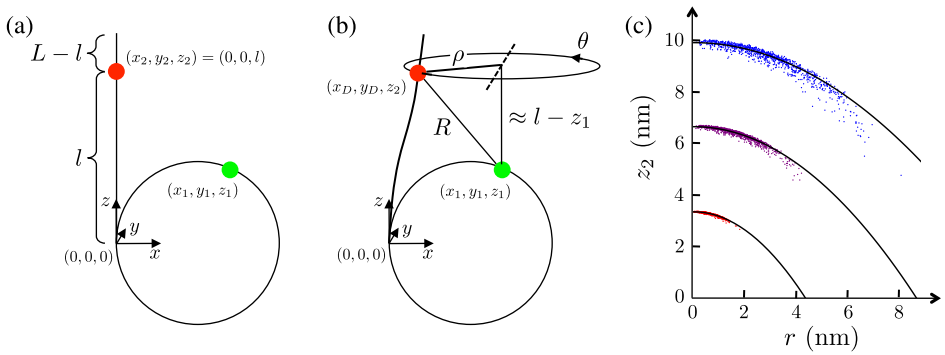

Figure 1. (*a*) Nucleosome with a straight unwrapped DNA portion. (*b*) Same as in (*a*) but with DNA bent. The depicted shape fluctuation shortens the distance between donor (green) and acceptor (red), thereby increasing the FRET efficiency. (*c*) Relation between z_2, the z-position of the acceptor, and r, its distance from the z-axis for $l = 10$ bp (red), $l = 20$ bp (purple) and $l = 30$ bp (blue). Comparison between Monte Carlo simulation (dots, 1000 realisations each) and theory, equation (9).

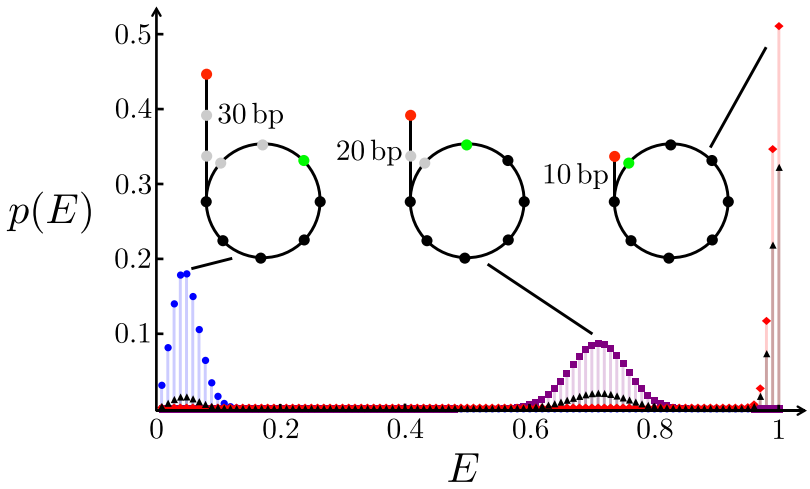

Figure 2. FRET efficiency distribution for three different amounts of unwrapping: 10 bp (red diamonds), 20 bp (purple squares) and 30 bp (blue circles); we disregard here the fully wrapped state. The corresponding geometry of the nucleosomal DNA is schematically indicated above each peak indicating the location of donor (green circle) and acceptor (red circle). Also shown is the combined FRET efficiency for the three unwrapped states (black triangles) assuming that the opening of each binding site (small circles in the nucleosomes) costs an extra amount of $1\,k_BT$. The broadening of the lines is calculated assuming bursts of 100 photons. In this plot we do not account for the shape fluctuations of the unwrapped DNA portion. As we shall demonstrate, these shape fluctuations have a dramatic impact on the FRET efficiency distribution, see figure 4(*b*).

when a sufficient amount of DNA is unwrapped the distance between donor and acceptor is too large for FRET to occur. As a result the observed distribution of FRET efficiencies is typically bimodal with a peak close to one (closed nucleosome) and a peak close to zero (open nucleosome).

In this paper we ask the question whether it is theoretically possible to have more than two peaks. Specifically, we calculate here the distribution of FRET efficiencies in an ideal experiment that does not suffer from the typical problems of an experimental setup (shot noise, flexible attachments of dyes, label stoichiometry, detection efficiencies, dye quantum yields, donor fluorescence leakage in the acceptor channel, direct excitation of the acceptor and many more). The setup we have in mind is depicted in figure 1(*a*) and is close to the one used in the experiments reported in [21]. When the DNA is fully wrapped the dyes are close to each other since they are just one helical turn apart: their distance is about 2.5 nm. The FRET efficiency follows from the distance R between donor and acceptor via the relation

$$E = \frac{1}{1 + (R/R_0)^6} \tag{1}$$

with $R_0 = 6.5$ nm [22]. With the opening of each binding site, the distance of the dyes grows; the geometrical details are given further below in this paper. For one binding site open, i.e., 10 bp unwrapped, we estimate a distance of about 2.8 nm and a FRET efficiency $E = 0.99$. For two binding sites open, or 20 bp unwrapped, the distance has grown to 5.6 nm and the efficiency is now $E = 0.71$. For three binding sites open, or 30 bp unwrapped, the distance is 10.6 nm and the efficiency has dropped to $E = 0.05$. For simplicity we will disregard in this study states with more than three open binding sites as they rarely occur [2, 7].

In figure 2 we show the expected distribution of FRET efficiencies for the first 3 unwrapping states. In this plot we accounted for a broadening of the peaks as expected for a finite number of photon counts per burst, here assumed to be 100, a typical value encountered in single-pair FRET experiments [21]. The distribution for each distance is then given by an appropriate binomial distribution [26]. We show both the distribution for pure states with a fixed amount of unwrapping (10 bp (red diamonds), 20 bp (purple squares) and 30 bp (blue circles)) as well as a combined efficiency where we assume following [7] that the opening of each binding site costs $1\,k_\mathrm{B}T$ (black triangles). Even in the latter case one can clearly distinguish three different unwrapping states with three different FRET efficiencies.

This raises the question why there are no clear signals for states with intermediate FRET values in the experiments [21]. We will show that, even in an ideal experimental setup, it is practically impossible to see such a signal. This is due to the shape fluctuations of the unwrapped portion of the DNA molecule. This might be surprising as the length of the intermediate unwrapped state is only 20 bp, much smaller than the persistence length of about 150 bp. However, the very sharp decay of the FRET efficiency around the distance R_0, see equation (1), leads to an extreme broadening of the DNA shape fluctuations in the FRET efficiency distribution.

In the following section we determine the shape fluctuations of the unwrapped portion of the DNA molecule. We first give an approximate analytical expression based on the continuous wormlike chain model and then test the quality of our prediction by a Monte Carlo simulation of a discrete chain. In section 3 we present the results, namely the distribution of dye–dye-distances for various unwrapping states of the nucleosome and the corresponding distributions of FRET efficiencies. We provide conclusions in section 4

2. Methods

Our goal is to determine the distribution of distances between a donor and an acceptor that result from shape fluctuations of the free portion of the DNA molecule, i.e. the part that is not adsorbed on the histone octamer, see figure 1(*b*), and how these fluctuations influence the FRET efficiency. In the next subsection we calculate the probability distribution for the position of the acceptor, which is assumed to be located on the unwrapped DNA portion, see figure 1, by modelling the DNA as a continuous wormlike chain. To make the calculation feasible we assume that the dye stays in the horizontal plane given by $z = z_2$. The quality of this assumption is checked afterwards by performing a Monte Carlo simulation of a discrete wormlike chain.

2.1. Shape fluctuations of the unwrapped DNA

We model the DNA as a wormlike chain with Hamiltonian

$$H = \frac{1}{2} k_\mathrm{B} T l_\mathrm{p} \int_0^L \left(\frac{\mathrm{d}\mathbf{u}(s)}{\mathrm{d}s} \right)^2 \mathrm{d}s \tag{2}$$

where l_p is the persistence length of DNA, L its contour length, s the coordinate along the DNA, and $\mathbf{u}$ the unit tangent vector along the DNA. At one end, at $s = 0$, the DNA is adsorbed to the histone octamer. We assume that this forces the tangent vector there to be constant and we choose $\mathbf{u}(0) = \mathbf{e}_z$ where $\mathbf{e}_z$ is the unit vector in the z-direction. We also choose the origin of our coordinate system at this adsorption point, see figure 1. In reality the adsorption potential is not infinitely narrow so the tangent vector at $s = 0$ might actually fluctuate as the actual position of the DNA varies. We neglect this effect since the positional fluctuations of the DNA at the binding sites are very small, on the order of 0.1 nm [1, 8, 27]. The other end of the DNA is free so we have

$$\left. \frac{\mathrm{d}\mathbf{u}}{\mathrm{d}s} \right|_{s=L} = 0. \tag{3}$$

We start by calculating the distribution of positions of a given point along the DNA at $s = l$ where $0 < l \leqslant L$. If there were no fluctuations this point would be at $l\mathbf{e}_z$ (this corresponds to the position of the acceptor in figure 1(*a*)). If we include fluctuations the distribution of positions is given by

$$G_t(\mathbf{r}) = \frac{\int \mathcal{D}[\mathbf{u}]\, \delta(\mathbf{r} - \int_0^l \mathbf{u}\mathrm{d}s) \mathrm{e}^{-\frac{H}{k_\mathrm{B}T}}}{\int \mathcal{D}[\mathbf{u}]\, \mathrm{e}^{-\frac{H}{k_\mathrm{B}T}}}, \tag{4}$$

see [28, 29]. The DNA we consider is short so fluctuations are small and we write

$$\mathbf{u} \approx u_x \mathbf{e}_x + u_y \mathbf{e}_y + \left(1 - \frac{1}{2}u_x^2 - \frac{1}{2}u_y^2\right) \mathbf{e}_z \tag{5}$$

where $u_x, u_y \ll 1$. We follow [28] and expand the Hamiltonian H, the argument of the δ-function, and the measure to second order in u_x and u_y. We then expand u_x and u_y in a sine-series, taking into account the boundary conditions:

$$u_x = \sum_{k_x=0}^{\infty} a_{k_x} \sin\left(\frac{(2k_x + 1)\,\pi s}{2L} \right) \tag{6}$$

and a similar equation for u_y. The delta function in equation (4) can be written as the product of three delta functions: one in the x-direction, one in the y-direction, and one in the z-direction. The delta function in the z-direction makes an analytic calculation of $G_t(\mathbf{r})$, within our approximation, hard if not impossible. Thus we calculate $G(x, y) = \int G_t(\mathbf{r})\,\mathrm{d}z$ instead. In fact, due to the rotational symmetry around the z-axis G only depends on the distance $r = \sqrt{x^2 + y^2}$ from the z-axis.

We use $2\pi\delta(t) = \int \exp(\mathrm{i}qt)\,\mathrm{d}q$ to calculate $G(r)$:

$$G(r) \approx \frac{3l_\mathrm{p}}{2\pi l^3} \exp\left(-\frac{3l_\mathrm{p} r^2}{2l^3} \right), \tag{7}$$

see [30] for details. Note that $G(r)$ does not depend on L but only on l. The average distance to the z-axis is

$$\frac{\langle r \rangle}{l} \approx \sqrt{\frac{\pi l}{6 l_\mathrm{p}}} \tag{8}$$

which shows that even for $l \ll l_\mathrm{p}$ the fluctuations can be considerable. For instance, if we take $l = 0.1 l_\mathrm{p}$ then $\langle r \rangle / l \approx 0.2$.

Along similar lines we calculate the average z-position for a given value of r:

$$\frac{\langle l - z(r)\rangle}{l} \approx \frac{l}{10l_\mathrm{p}}\left(1 + \frac{6l_\mathrm{p}r^2}{l^3}\right). \tag{9}$$

This formula is very accurate as a comparison to Monte Carlo simulations (described in the next section) shows, see figure 1(*c*) where $z_2 = \langle z(r)\rangle$, except for some deviations for rare large deformations where equation (9) overestimates $\langle z(r)\rangle$. Just to get an idea, for $r = \sqrt{2l^3/(3l_\mathrm{p})}$ the function $G(r)$ has dropped by $1/e$ compared to its value at $r = 0$. One has then an average shortening by $\langle l - z(r)\rangle = l^2/(2l_\mathrm{p})$. As long as $l \ll l_\mathrm{p}$ this shortening is very small, e.g. about 0.1 nm for 10 bp and still only about 1 nm for 30 bp. To estimate the range of z-positions at given r we also give here the second moment

$$\sqrt{\langle (l - z(r))^2\rangle - \langle l - z(r)\rangle^2} = \frac{l^2}{10l_\mathrm{p}}\sqrt{\frac{2}{7}\left(1 + \frac{2l_\mathrm{p}r^2}{l^3}\right)}. \tag{10}$$

This shows that fluctuations in z at fixed r are very small; e.g. for $r = \sqrt{2l^3/(3l_\mathrm{p})}$ they are given by $\sqrt{2/3}\,l^2/(10l_\mathrm{p})$.

2.2. Monte Carlo simulation

In the next section we calculate the donor-acceptor distance distribution. In the calculation (more specifically, in equation 14 below) we neglect the change in z-position of the fluorophore that is attached to the DNA due to fluctuations of the DNA, see also figure 1(*b*). We check the quality of this approximation numerically by generating configurations of the unwrapped DNA portion according to the Boltzmann distribution, with the energy given by equation (2), calculating the distance between the two fluorophores for each configuration, and then binning the results to get the fluorophore distance distribution.

More specifically, the DNA is modelled as a chain consisting of N segments of length $a = L/N$ and of direction $\mathbf{t}_i$, $i = 1, ..., N$. The Hamiltonian is a discretised version of equation 2

$$H = \frac{\overline{\kappa}}{a}\sum_{i=1}^{N-1}(1 - \mathbf{t}_i \cdot \mathbf{t}_{i+1}) \tag{11}$$

where $\overline{\kappa}$ is given by

$$I_{3/2}\left(\frac{\overline{\kappa}}{ak_\mathrm{B}T}\right) = I_{1/2}\left(\frac{\overline{\kappa}}{ak_\mathrm{B}T}\right)\mathrm{e}^{-a/l_\mathrm{p}}, \tag{12}$$

see [28]. For small enough segment lengths, $\overline{\kappa}$ approaches the bending modulus κ that is related to the persistence length l_p via $l_\mathrm{p} = \kappa/k_\mathrm{B}T$. We take $\mathbf{t}_1 = (0, 0, 1)$ and generate a DNA chain by randomly generating values for $\cos\gamma_i \equiv \mathbf{t}_i \cdot \mathbf{t}_{i+1}$, $i = 1, ..., N-1$. More specifically, for segment i we choose a bending direction ϕ_i randomly from $[0, 2\pi]$ and we draw a random bending angle γ_i from the distribution $\rho(\gamma_i) \propto \gamma_i \exp\left(-l_\mathrm{p}\gamma_i^2/(2a)\right)$. We choose N to be sufficiently large so that the segment length a is short enough to use this distribution instead of the exact distribution $\rho(\gamma_i) \propto \gamma_i \exp\left(\overline{\kappa}\cos\gamma_i/(ak_\mathrm{B}T)\right)$.

In our Monte Carlo simulation we generate many of these chains and measure the distance from the donor to the acceptor to obtain a distribution of distances. We determined for each of the three lengths ($l = L = 10$, 20 and 30 bp) the minimum number of segments necessary to have results that do not depend on N anymore and found it to be 50. For smaller N-values the peaks are sharper (for $N = 4$ the peak is about 20% higher and for $N = 10$ about 5% higher for all three unwrapping lengths). In the results shown in the next section, we used $N = 75$ segments and 500 000 realisations for each unwrapping length.

3. Results

3.1. Donor-acceptor distance distribution

To calculate the distribution of FRET efficiencies we need to determine the distribution of donor and acceptor distances first. We assume that the DNA is wrapped along a circle of radius $r_0 = 4.3$ nm that lies in the xz-plane in figure 1. This is a reasonable assumption since the outer parts of the wrapped DNA portion have a pitch angle close to zero [1]. The fluorophore on the wrapped part (shown in green in figure 1) is positioned at $\mathbf{r}_1 = x_1\mathbf{e}_x + y_1\mathbf{e}_y + z_1\mathbf{e}_z$ where we assume (independent of the unwrapping state) that $y_1 = 2.5$ nm. The unwrapped portion of the DNA lies on the z-axis in the absence of shape fluctuations, see figure 1(*a*). The fluorophore on the unwrapped portion (shown in red in figure 1) is at position $\mathbf{r}_2 = z_2\mathbf{e}_z$ (since $x_2 = y_2 = 0$). With the opening of each binding site the length of the unwrapped portion increases by 10 bp. We keep y_1, x_2 and y_2 fixed and set $z_2 = n \times 3.4\,\mathrm{nm} = l$, $x_1 = r_0[1 - \cos(z_2/r_0)]$ and $z_1 = r_0\sin(z_2/r_0)$ where n denotes the number of open binding sites.

We calculate the distance distribution under the simplifying assumption that the fluorophore on the DNA stays in the plane $z = z_2 = l$ when the DNA fluctuates. Later we compare these results, which are obtained analytically, to numerical calculations that do not make this assumption.

As we saw in the previous section, the probability for the centre of the DNA at $l = z_2$ to be at $x = x_D$ and $y = y_D$ is

$$G(x_D, y_D) = \frac{3l_\mathrm{p}}{2\pi l^3}\exp\left(-\frac{3l_\mathrm{p}\left(x_D^2 + y_D^2\right)}{2l^3}\right). \tag{13}$$

The position of the fluorophore is then $x = x_D$ and $y = y_D$, and the distance R between the donor and the acceptor is

$$R = \sqrt{(x_D - x_1)^2 + (y_D - y_1)^2 + (l - z_1)^2}. \tag{14}$$

Now let us choose $x_D = x_1 + \rho\sin\theta$ and $y_D = y_1 + \rho\cos\theta$ where $\rho = \sqrt{R^2 - (l - z_1)^2}$. The Jacobian for the transformation from (x_D, y_D) to (ρ, θ) is ρ so the distribution of ρ-values G_ρ is

$$\begin{aligned} G_\rho(\rho) &= \int_0^{2\pi} G(x_1 + \rho\sin\theta, y_1 + \rho\cos\theta)\,\rho\,\mathrm{d}\theta \\ &= \frac{3l_\mathrm{p}\rho}{l^3}\exp\left(-\frac{3l_\mathrm{p}\left(\rho_0^2 + \rho^2\right)}{2l^3}\right) I_0\left(\frac{3l_\mathrm{p}\rho_0\rho}{l^3}\right) \end{aligned} \tag{15}$$

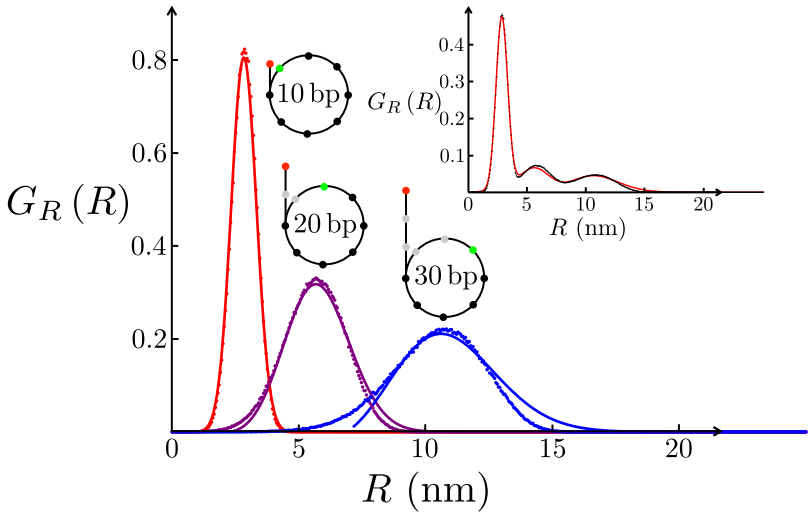

Figure 3. Distribution of donor-acceptor distances for three different amounts of unwrapping. Comparison between the analytical expression (solid lines), equation (16), and the result from the Monte Carlo simulation (dots). The inset shows the combined distribution of distances for the three states, assuming a one k_BT cost for opening of binding sites (red curve: analytical expression, black dots: Monte Carlo simulation).

where I_0 is the modified Bessel function of the first kind of order 0, and where $\rho_0 = \sqrt{x_1^2 + y_1^2}$ is the value of ρ when the DNA does not fluctuate, i.e. when $x_D = y_D = 0$. Since $\rho = \sqrt{R^2 - (l - z_1)^2}$ and thus $R\,\mathrm{d}R = \rho\,\mathrm{d}\rho$ the distribution of donor-acceptor distances G_R can easily be calculated from equation 15, namely

$$G_R(R) = \frac{3l_p R}{l^3} \mathrm{e}^{-3l_p\left(R^2-(l-z_1)^2+\rho_0^2\right)/2l^3} I_0\left(\frac{3l_p\rho_0}{l^3}\sqrt{R^2-(l-z_1)^2}\right). \quad (16)$$

In figure 3 we show the distribution of donor-acceptor distances for three different amounts of unwrapping. This plot compares the analytical expression, equation (16) with the results from the Monte Carlo simulation. The positions of the maxima and the full widths at half maximum agree well for all three unwrapping length (largest deviations for $l = 30$ bp: theoretical peak position shifted by 0.1 nm compared to simulation but same full width at half maximum). However, with increasing length there is a systematic deviation that shows that the analytical expression underestimates the distribution for shorter distances and overestimates it for larger differences. This reflects our approximation $z_2 = l$: for strong bending of the free DNA one expects a shortening in the z-direction, see figure 1(c), manifesting itself in the systematic shift in the distribution. Still, the theoretical expression gives a reasonable description even for 30 bp. The inset in figure 3 shows the overall distribution of distances under the assumption that the net energy per binding site is 1 k_BT [7], i.e., that the state with n open binding sites occurs with a probability $p \sim \mathrm{e}^{-n}$. Note that also this combined distribution shows three clear peaks corresponding to the three unwrapping states. As we shall see in the next subsection this clear picture disappears once we look at the distribution of FRET efficiencies.

3.2. FRET efficiencies

Here we calculate the FRET efficiency $p(E)$ from the distribution of dye–dye distances $G_R(R)$. To do so we need to combine equations (1) and (16). First we solve equation (1) for R leading to $R(E) = R_0((1-E)/E)^{1/6}$. Then $p(E)$ follows from

$$G_R(R)\,\mathrm{d}R = G(R(E))\left|\frac{\mathrm{d}R}{\mathrm{d}E}\right|\mathrm{d}E = p(E)\,\mathrm{d}E. \quad (17)$$

This leads to

$$p(E) = \frac{l_p R_0^2}{2l^3E^2}\left(\frac{E}{1-E}\right)^{2/3} \mathrm{e}^{-3l_p\left(R_0^2\left(\frac{1-E}{E}\right)^{1/3}-(l-z_1)^2+\rho_0^2\right)/2l^3} I_0\left(\frac{3l_p\rho_0}{l^3}\sqrt{R_0^2\left(\frac{1-E}{E}\right)^{1/3}-(l-z_1)^2}\right). \quad (18)$$

The distribution of FRET efficiencies is depicted in figure 4(a) for the first three states of unwrapping. The state with 10 bp unwrapped shows a sharp signal peaked very close to $E = 1$ whereas for 30 bp unwrapped one finds a peak close to $E = 0$. This is in sharp contrast to the signal that we predict for the 20 bp state. Even for the ideal experimental situation assumed here, one does not find a clear peak but instead the distribution is smeared out over nearly the whole range of E-values. This reflects the fact that in this case the dye–dye distance is peaked close to the Förster radius $R_0 = 6.5$ nm. As the unwrapped DNA portion fluctuates, it brings the dyes in and out of that distance. With the strong dependence of E on R around R_0, see equation (1), nearly the whole range of efficiencies is attained. That the shape fluctuations have such a huge effect on the FRET signal is somewhat surprising as the unwrapped DNA segment is only 20 bp long, much shorter than the DNA persistence length of about 150 bp.

The combined FRET efficiency for all three unwrapping states is plotted in figure 4(b), again under the assumption

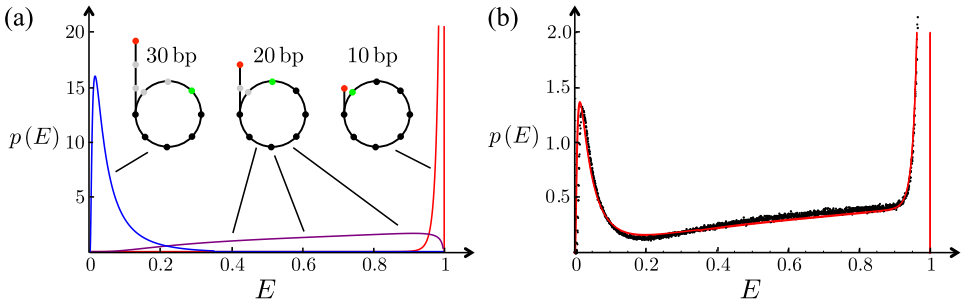

Figure 4. (*a*) FRET efficiencies of the first 3 unwrapping states. (*b*) Combined FRET efficiencies where the three unwrapping states are Boltzmann weighted assuming that each unspooling step cost $1\,k_BT$. Comparison between theory (red curve) and simulation (black dots), see also inset of figure 3 for the corresponding distribution of donor-acceptor distances.

that each unwrapping step costs $1\,k_BT$. This looks vastly different from the corresponding distribution of distances, see the inset of figure 3. The FRET signal shows two clear peaks connected by a broad shoulder that stems from the 20 bp state. A comparison with experimental data, e.g. in [20] or [21], is difficult due to various experimental complications. It is, however, clear from our theoretical analysis that even in the absence of these complications the distribution of FRET efficiencies for each state, figure 4(*a*), is very different from Gaussian, unlike the distribution of distances between the donor and acceptor, figure 3. A simple geometrical model that does not account for DNA shape fluctuations like the one presented in [20] is useful to learn about the possible states of the system but might suggest a wrong picture for the distribution of intermediate FRET efficiencies.

4. Conclusion

We have calculated the effect of DNA fluctuations on the distribution of the donor-acceptor distance in a typical FRET experiment that studies site exposure in nucleosomes. We found that the FRET method as a quantitative molecular ruler is seriously hampered by the steep decay of the FRET efficiency with distance over a very short range. On the one hand, this means that one can detect easily two populations of nucleosome states: open and closed. On the other hand, it is impossible to obtain a clearly peaked intermediate FRET signal since it will be smeared out by DNA shape fluctuations over nearly the whole range of FRET values. To learn more about nucleosomal states than just the binary information 'open' versus 'closed' one needs to work with various constructs where in each case the dyes are placed at strategic positions as has been done for example in [21].

Acknowledgments

We thank J van Noort, M Tompitak and B Eslami-Mossallam for fruitful discussions. This work is part of the research programme of the Foundation for Fundamental Research on Matter (FOM), which is financially supported by the Netherlands Organisation for Scientific Research (NWO). HS is grateful for the hospitality of KITP, where part of this work was completed.

References

[1] Luger K, Mäder A W, Richmond R K, Sargent D F and Richmond T J 1997 *Nature* **389** 251–60
[2] Polach K J and Widom J 1995 *J. Mol. Biol.* **254** 130–49
[3] Anderson J D and Widom J 2000 *J. Mol. Biol.* **296** 979–87
[4] Anderson J D and Widom J 2001 *Mol. Cell. Biol.* **21** 3830–9
[5] Anderson J D, Lowary P T and Widom J 2001 *J. Mol. Biol.* **307** 977–85
[6] Anderson J D, Thaström A and Widom J 2002 *Mol. Cell. Biol.* **22** 7147–57
[7] Prinsen P and Schiessel H 2010 *Biochimie* **92** 1722–8
[8] Schiessel H 2014 *Biophysics for Beginners: A Journey Through the Cell Nucleus* (Singapore: Pan Stanford)
[9] Li G and Widom J 2004 *Nature Struct. Mol. Biol.* **11** 763–9
[10] Li G, Levitus M, Bustamante C and Widom J 2005 *Nature Struct. Mol. Biol.* **12** 46–53
[11] Tims H S, Gurunathan K, Levitus M and Widom J 2011 *J. Mol. Biol.* **411** 430–48
[12] Böhm V, Hieb A R and Andrews A J, Gansen A, Rocker A, Tóth K, Luger K and Langowski J 2011 *Nucl. Acids Res.* **39** 3093–102
[13] Moyle-Heyrman G, Tims H S and Widom J 2011 *J. Mol. Biol.* **412** 634–46
[14] Tóth K, Böhm V, Sellmann C, Danner M, Hanne J, Berg M, Barz, I, Gansen A and Langowski J 2013 *Cytometry* A **83** 839–46
[15] Tomschik M, Zheng H, van Holde K, Zlatanova J and Leuba S H 2005 *Proc. Natl Acad. Sci. USA* **102** 3278–83
[16] Kelbauskas L, Chan N, Bash R, Yodh J, Woodbury N and Lohr D 2007 *Biochemistry* **46** 2239–48
[17] Kelbauskas L, Sun J, Woodbury N and Lohr D 2008 *Biochemistry* **47** 9627–35
[18] Kelbauskas L, Woodbury N and Lohr D 2009 *Biochem. Cell Biol.* **87** 323–35
[19] Gansen A, Toth K, Schwarz N and Langowski J 2009 *J. Phys. Chem.* B **113** 2604–13
[20] Gansen A, Valeri A, Hauger F, Felekyan S, Kalinin S, Toth K, Langowski J and Seidel C A M 2009 *Proc. Natl Acad. Sci. USA* **106** 15308–13
[21] Koopmans W J A, Buning R, Schmidt T and van Noort J 2009 *Biophys. J.* **97** 195–204
[22] Buning R and van Noort J 2010 *Biochimie* **92** 1729–40
[23] Lee J Y and Lee T-H 2012 *Biochim. Biophys. Acta* **1824** 974–82
[24] Jimenez-Useche I and Yuan C 2012 *Biophys. J.* **103** 2502–12
[25] Gansen A, Hieb A R, Böhm V, Tóth K and Langowski J 2013 *Plos One* **8** e57018

[26] Nir E, Michalet X, Hamadani K M, Laurence T A, Neuhauser D, Kovchegov Y and Weiss S 2006 *J. Phys. Chem.* B **110** 22103–24
[27] Fathizadeh A, Besya A B, Ejtehadi M R and Schiessel H 2013 *Eur. Phys. J.* E **36** 21
[28] Wilhelm J and Frey E 1996 *Phys. Rev. Lett.* **77** 2581–4
[29] Kulić I M, Mohrbach H, Thaokar R and Schiessel H 2007 *Phys. Rev.* E **75** 011913
[30] Kleinert H 2009 *Path Integrals in Quantum Mechanics, Statistics, Polymer Physics, and Financial Markets* (Singapore: World Scientific)